Supplementary Information

Preparation of size tunable giant vesicles from cross-linked dextran(ethylene glycol) hydrogels

Néstor López Mora,[a] Jesper S. Hansen,[b] Yue Gao,[a] Andrew A. Ronald,[b] Roxanne Kieltyka,[a] Noah Malmstadt,[b]* and Alexander Kros[a]*

[a]Soft Matter Chemistry, Leiden Institute of Chemistry, Leiden University, P.O. Box 9502, 2300 RA Leiden, The Netherlands.

[b]Mork Family Department of Chemical Engineering and Materials Science, University of Southern California, Los Angeles, CA 90007.

TABLE OF CONTENT

MATERIALS

Cholesterol (CH), 1,2-dioleoyl-sn-glycero-3-phosphocholine (DOPC), 1,2-dioleoyl-sn-glycero-3-phosphoethanolamine (DOPE), 1-palmitoyl-2-oleoyl-sn-glycero-3-phosphocholine (POPC), 1-palmitoyl-2-oleoyl-sn-glycero-3-phospho-(1'-rac-glycerol) (sodium salt) (POPG), 1,2-dioleoyl-sn-glycero-3-phosphoethanolamine-N-[methoxy(polyethylene glycol)-2000] (ammonium salt) (PEG2000-PE), 1,2-dioleoyl-sn-glycero-3-phosphoethanolamine-N-(lissamine rhodamine B sulfonyl) (ammonium salt) (PE-LR) were purchased from Avanti Polar Lipids. 1,2-dipalmitoyl-sn-glycero-3-phosphocholine (DPPC), 4-nitrophenyl disulfide, 4-(dimethylamino) pyridine (DMAP), 1500 and 3400 Da poly (ethylene glycol) dithiol (PEGDT), 7-methoxycoumarin-3-carboxylic acid, and 4-(2-Hydroxyethyl)piperazine-1-ethanesulfonic acid, N-(2-Hydroxyethyl) piperazine-N′-(2-ethanesulfonic acid) (HEPES) were purchased from Aldrich. Maleic anhydride, N,N'-Diisopropylcarbodiimide (DIC), p-toluene sulfonic acid monohydrate (PTSA) and maleimide were purchased from Fluka. Dextran (Mn = 2 000, 70 000 and, 150 000, Pharmacia Fine Chemicals, Sweden) was dried in the vacuum oven for several days before use. N-Maleoyl-β-alanine was synthesized according to a reported procedure.[1] 4-(Dimethylamino) pyridinium 4-toluenesulfonate (DPTS) was synthesized from DMAP and PTSA.[2] Dextran Maleimide (Dex-Mal) was synthesized by esterification of the hydroxyl group of the dextran with N-Maleoyl-β-alanine.[3]

CHARACTERIZATION TECHNIQUES

Osmomolality was determined from the freezing point depression using an Osmometer Roebling Type 13. The Osmometer was calibrated using 100 mOsm/kg NaCl standard solution.

Fluorescence Microscopy was performed on a Zeiss axiovert-200 inverted microscope equipped with a Chroma TRITC and DAPI BP 445/50 fluorescence filter sets. Images were recorded with a black and white CCD camera (AxioCam NRm).

Confocal Imaging was performed in a TI-Eclipse inverted microscope (Nikon, Japan) equipped with a 16-bit Cascade II 512 EMCCD camera (Photometrics, USA). Spinning-disc confocal microscopy was performed using a CSUX confocal head (Yokogawa, Japan). Illumination was provided by a 50 mW solid-state laser at 561 nm

(Coherent Inc., Germany). Fluorescence was imaged through a bandpass filter centered at 595 nm. Epifluorescence was performed with a 40× objective and confocal microscopy was carried out using a 60× NA1.43 Plan-Apo Nikon oil-immersion objective.

Two photon microscopy was performed in a Bio-Rad 2100MP confocal and multi-photon microscope with inverted TE 2000U Nikon microscope. Fluorescence was imaged using a 20x Nikon objective (Plan Apo, NA 0.75). Illumination was provided by a 5-W Tsunami laser (Spectra Physics, Mountain View, CA, USA) with a range of 700 – 900 nm. The images were collected using Lasersharp 4.0 software by Biorad.

Fluorescence spectroscopy was performed on a FS920 Fluorometer (Edinburgh Instruments) equipped with a DTMS-300X excitation monochrometer and a peltier-controlled thermostatic cell. A quartz cuvette with a 1 cm path length was used. The excitation and emission slit widths were 1 nm. Scans were performed with steps of 0.5 nm, with a sampling time of 0.5 s per wavelength.

Contact angle. Drop shape analysis was made by using LBADSA plugin in ImageJ software.

Size distribution analysis was made by using Analyze Particles tool in ImageJ software.

EXPERIMENTAL

Synthesis of Dex-Mal. Dex-Mal (molecule **1**) was synthesized by DIC mediated esterification of the hydroxyl groups of dextran with N-Maleoyl-β-alanine. Briefly, N-Maleoyl-β-alanine (1 eq.), DPTS (0.15 eq.) and DIC (1.5 eq.) were dissolved in anhydrous DMSO. The mixture was stirred at room temperature for two hours, followed by adding the DMSO solution of Dextran (2.5 eq.). After overnight stirring at room temperature, the formed N, N'-dialkylurea was removed by filtration and the crude product was obtained by precipitation in cold isopropanol. The precipitate was dissolved in water and extensively dialyzed against Milli-Q water for two days and subsequently lyophilized. ^{1}H NMR (400 MHz, D2O): δ 3.3-4.0 (m, dextran glucopyranosyl ring protons), 4.9 (s, dextran anomeric proton), 6.8 (s, maleimide). The degree of substitution (DS) of Dex-Mal is defined as the number of maleimide groups per 100 glucopyranose residues of dextran, which was calculated from the ^{1}H NMR spectra based on the protons of maleimide (δ 6.8) and the anomeric proton (δ 4.9). The DS of Dex-PEG was controlled by the molar ratio between dextran and N-Maleoyl-β-alanine.

Synthesis of Dex-Mal-C. The covalently fluorescent labeled Dex-Mal (Dex-Mal-C) was synthesized by a similar procedure as Dex-Mal. Briefly, 7-methoxycoumarin-3-carboxylic acid (0.025 eq. or 0.05 eq.) was added together with N-Maleoyl-β-alanine (1 eq.), DPTS (0.15 eq.) and DIC (1.5 eq.) in anhydrous DMSO. Dextran (2.5 eq.) was also dissolved in anhydrous DMSO and added into the previous mixture. After overnight stirring at room temperature, the product was purified by filtration, precipitation and dialysis. All these steps were carried out in dark to prevent the bleaching of coumarin.

Glass slides functionalization. Cleaning and thiol surface modification (silanization) was performed according to a previously reported method.[4] Glass substrates were standard microscope glass slides (Menzel-Gläser) 76 x 26 mm.

Dex-PEG Hydrogel. Maleimide-modified Dextran (**1**) (2 % weight solution) was cross-linked by using PEG (**2**) in three different ratios (1 : 1, 1 : 0.75 and, 1 : 0.5) at room temperature. Typically, **1** (60 mg) (Degree of substitution = 4) was dissolved in water (2.5 g) and 11.11 mg of molecule **2** (1500 Da) in water (0.5 g) were mixed to provide a hydrogel solution in 1 : 1 molar ratio. The mixture was shaken in a vortex for 1 minute and immediately used for the substrate preparation.

Dex-PEG coated glass slides. A solution of 2% Dex-PEG (600 µL) was added onto the prepared thiol functionalized microscope glass slides. A homogenous polymeric film was formed after 30–45 minutes at 40 °C. The Dex-PEG coated microscope slides were stored for further use.

Lipid Mixtures. Each of the lipid mixtures used was made by mixing 14 mM lipid solutions of the individual various lipids together to obtain the indicated molar ratios and yield a final mixture of a 14 mM lipid solution (see below **Table S1**). Additionally 1,2 – dioleoyl – sn – glycerol – 3 – phosphoethanolamine – N - (lissamine rhodamine B sulfonyl) (ammonium salt) (PE-LR) was added to each lipid mixture in 0.5 molar % for the purpose of gathering fluorescence images. All lipid mixtures were stored at -20 °C until they were used.

GUVs formation. The desired lipids (10 µL) were spread out, using a micropipette, onto the Dex-PEG coated slides. Subsequently, the deposited lipid layer was dried for 30 minutes in a vacuum oven at 35 °C. The GUV growth chamber was made by placing a 15 mm (OD) glass O-Ring on top of the hydrogel and sealed with high vacuum silicon grease. Finally, the lipid film was swelled using the desired immersion media (300 µL).

RESULTS AND DISCUSSION

The characterization of functionalized microscope glass slides before and after silanization was made by drop shape analysis. Results for chemically cleaned and modified surfaces (***Figure S1***) showed an angle of 10 ± 1° before and 67 ± 4°. The remaining water content in the dry Dex-PEG film (contact angle = 26 ± 7°) was determined by weight lost. We found, after drying the hydrogel film at 110 °C overnight, a water content of 1.9 ± 0.14 % in the dry state. The water uptake of the Dex-PEG hydrogel film was determined by weight increase. Dex-PEG functionalized microscope glass slides were immersed in 1x PBS and the weight was taken every hour. The water uptake content against time is plotted in ***Figure S2***. Those results indicate that the hydrogel film in the wet state takes up to 89 % PBS buffer during swelling after one hour and then stays constant. This high swelling efficiency produces the forces normal to lipid bilayers that promote the growing of GUVs, without addition of any non-electrolytic monosaccharaides to promote lamellar repulsion.

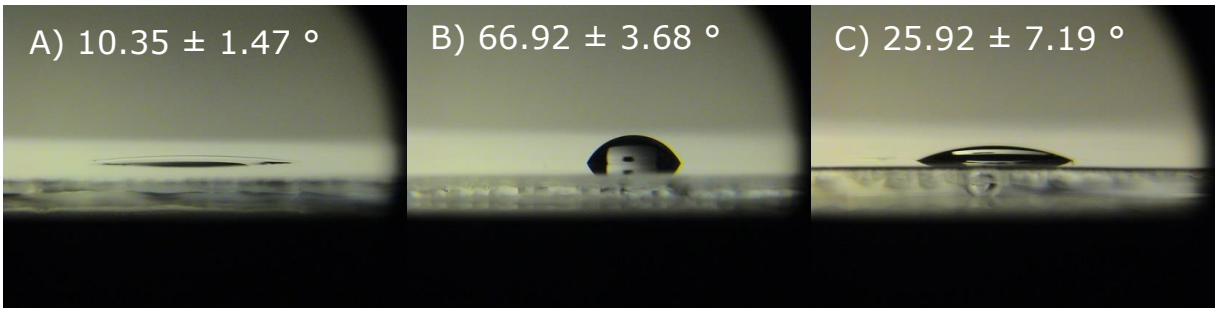

Figure S1. Contact angle measurements for A) Microscope glass slide after cleaning, B) Microscope glass slide after silanization and, C) Microscope glass slide after Dex-PEG hydrogel coating.

GUVs were growth in two different immersion media: PBS and HEPES Potassium Chloride saline (HBS) buffers. All lipid compositions (see **Table S1**) were tested in PBS and HBS growth buffers. The vesicle diameter is the average of measuring between 50 to 100 different GUVs in PBS buffer. GUVs smaller than 1 μm cannot be resolved due to they are below the resolution limit of optical microscopy. Lipid mixtures (A–I) were prepared in 95 chloroform : 5 methanol % volume at 14 mM. PE-LR was used as fluorescent probe in 0.5 % mol (A–F and I) or 0.1 % mol (G, H) concentration. Results for all different tested lipid compositions are presented in ***Figures S3, S5, S7, S9, S11, S13, S14, S15,*** and ***S17***. In the left side results for GUVs growth in PBS and right side in HBS. All images were taken from free floating vesicles after waiting 30 minutes in order to allow them to sink in the

bottom of the observation chamber. Imaging of GUVs was made using 20x (top image) and 63x (bottom image) objectives in fluorescence microscopy mode. Comparing qualitatively the sizes of GUVs in those two different immersion media, the diameter size of GUVs was bigger when the immersion media was HBS than in PBS. Additionally, quantitative size distribution analysis was performed by counting GUVs that were grown in PBS buffer during one hour (***Figures S4, S6, S8, S10, S12*** and ***S16***).

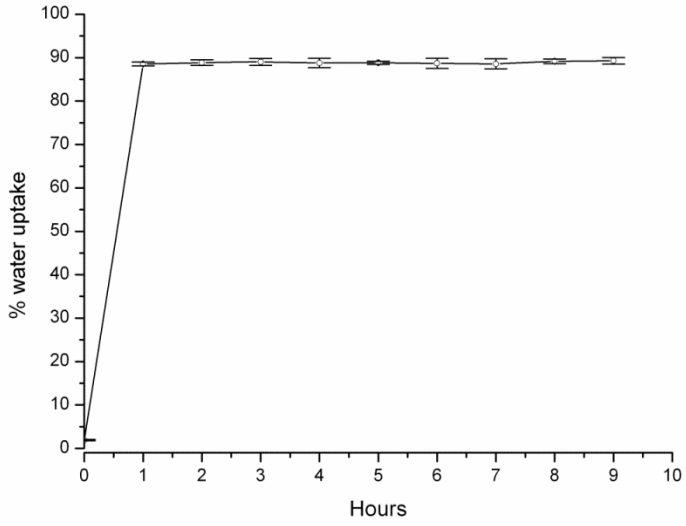

Figure S2. Water uptake in a Dex-PEG hydrogel film after 9 hours of swelling in 1x PBS buffer.

Table S1. **Lipid compositions tested for GUVs growth on Dex-PEG at physiological ionic strength (>300 mOsm/kg).**

	Lipid composition (% mol)	PBS	HBS	Diameter (μm)	Figure
A	90% POPC / 10% CH	√	√	12.62 ± 5.89	S3
B	80% POPC / 20% CH	√	√	9.38 ± 5.04	S5
C	90% POPC / 10% POPG	√	√	12.19 ± 4.75	S7
D	50% POPC / 50% POPG	√	√	14.45 ± 7.51	S9
E	90% POPC / 10% DOPS	√	√	9.80 ± 3.50	S11
F	50% DOPC / 25% DOPE / 25% CH	√	√	11.62 ± 5.35	S13
G	50% DOPC / 50% DPPC	√	√	N.D.	S15
H	33.3% DOPC / 33.3% DPPC / 33.3% CH	√	√	N.D.	S16
I	50% DOPC / 20% DOPE / 5% PEG2000-PE / 25% CH	√	√	N.D.	S17

N.D. represents not determined.

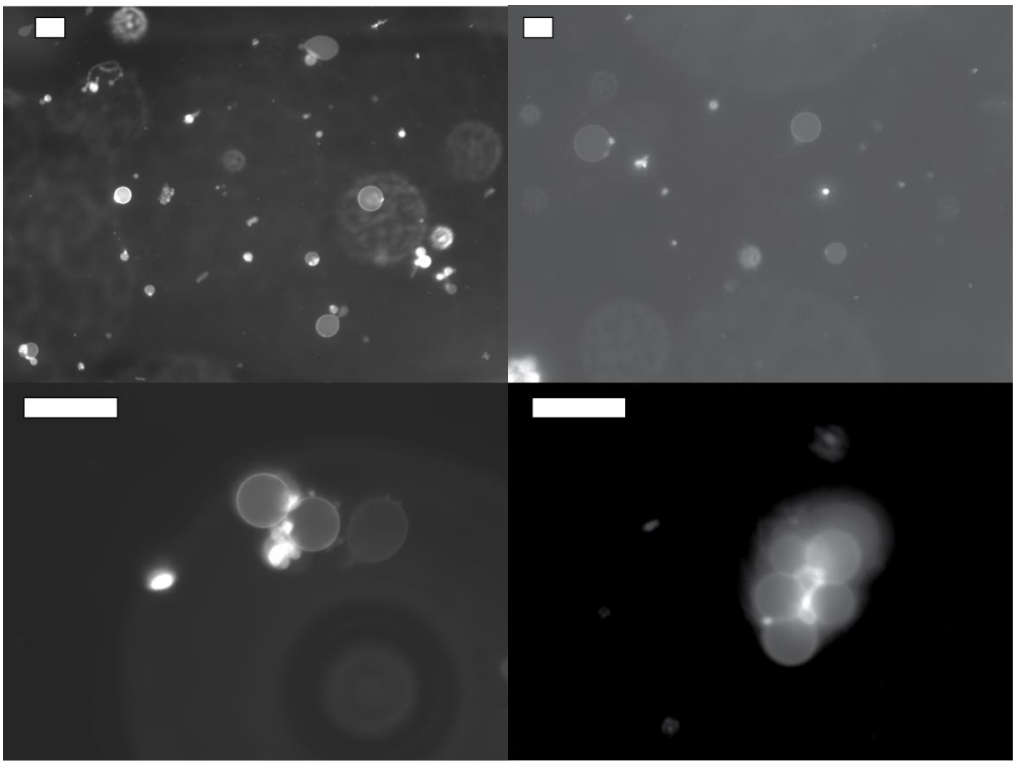

Figure S3. Free floating GUVs formed from **A** (90% POPC / 10% CH) in PBS left column and HBS right column. On top 20x magnification and, bottom 63x magnification. The scale bars are 50 μm.

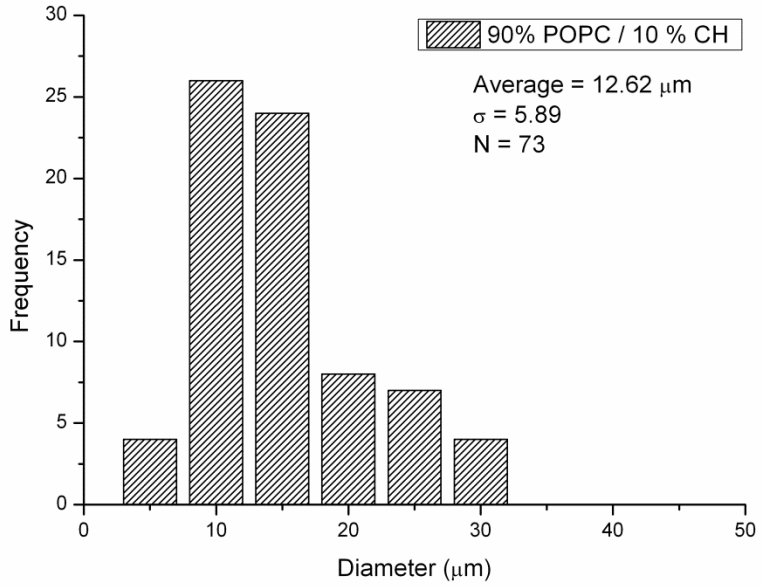

Figure S4. Size distribution of GUVs with lipid composition **A** (90% POPC / 10% CH) in PBS.

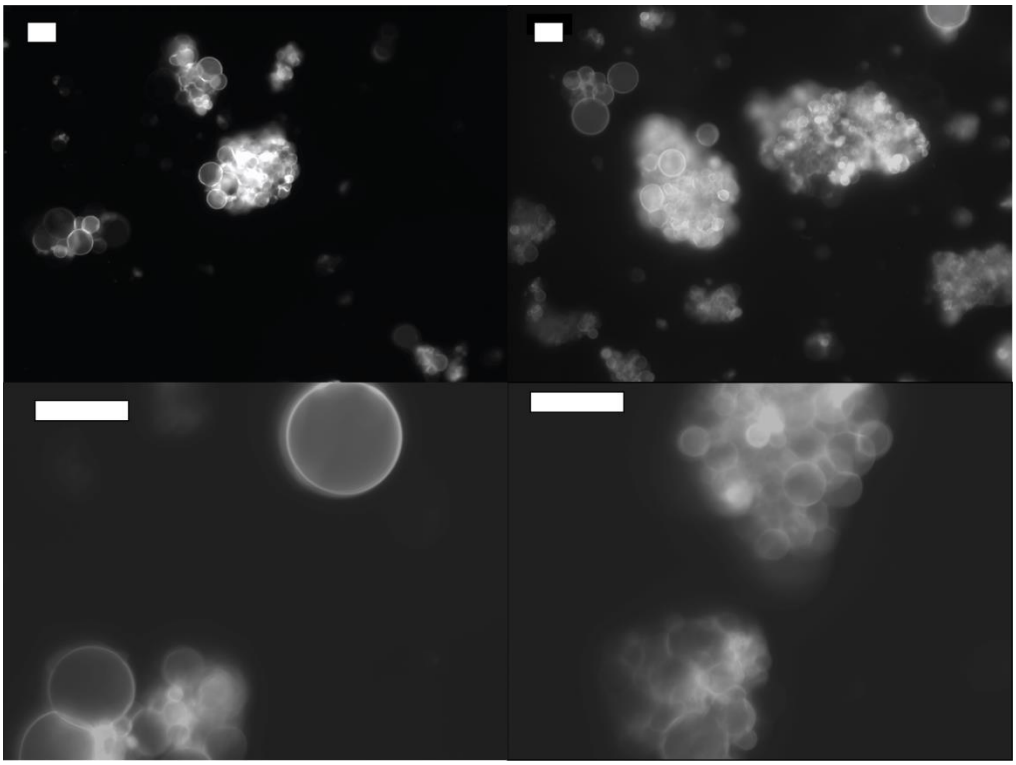

Figure S5. Free floating GUVs formed from **B** (80% POPC / 20% CH) in PBS left column and HBS right column. On top 20x magnification and, bottom 63x magnification. The scale bars are 50 μm.

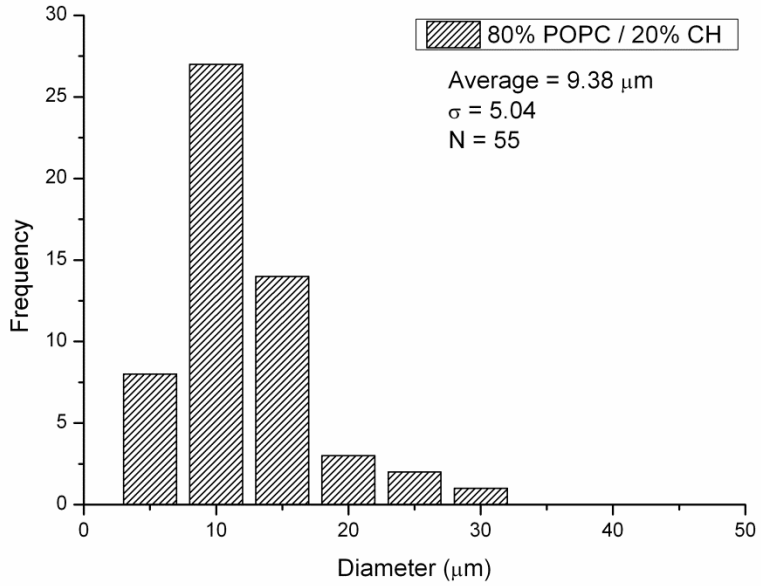

Figure S6. Size distribution of GUVs with lipid composition **B** (80% POPC / 20% CH) in PBS.

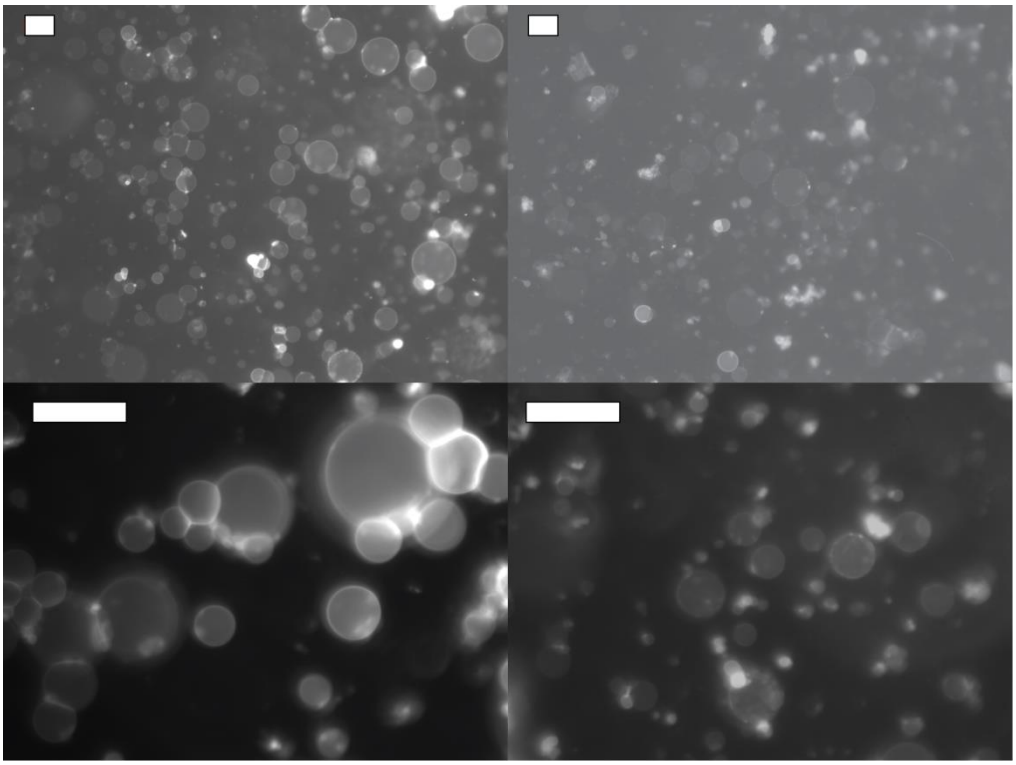

Figure S7. Free floating GUVs formed from **C** (90% POPC / 10% POPG) in PBS left column and HBS right column. On top 20x magnification and, bottom 63x magnification. The scale bars are 50 μm.

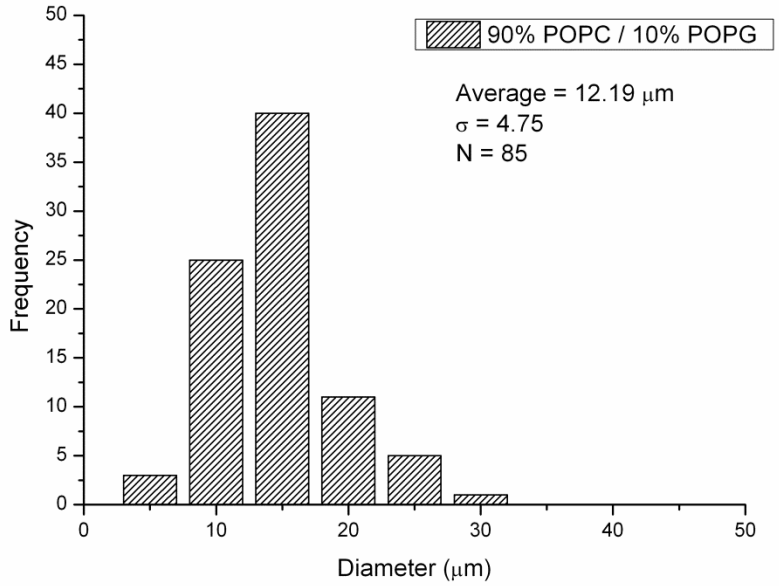

Figure S8. Size distribution of GUVs with lipid composition **C** (90% POPC / 10% POPG) in PBS.

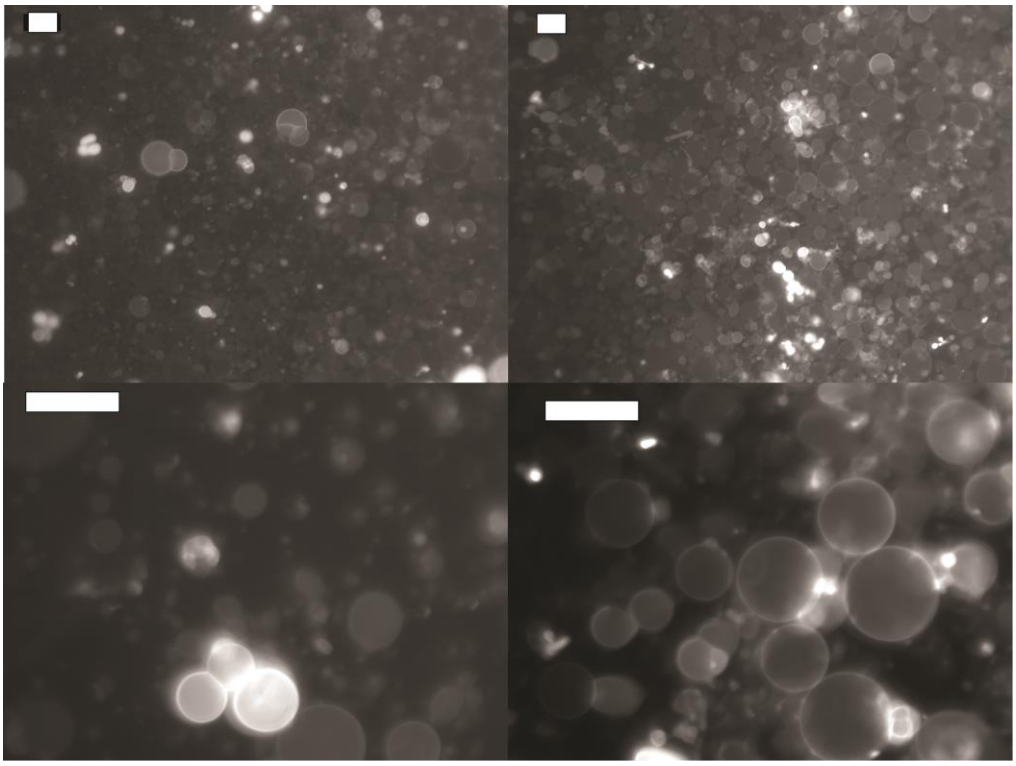

Figure S9. Free floating GV formed from **D** (50% POPC / 50% POPG) in PBS left column and HBS right column. On top 20x magnification and, bottom 63x magnification. The scale bars are 50 μm.

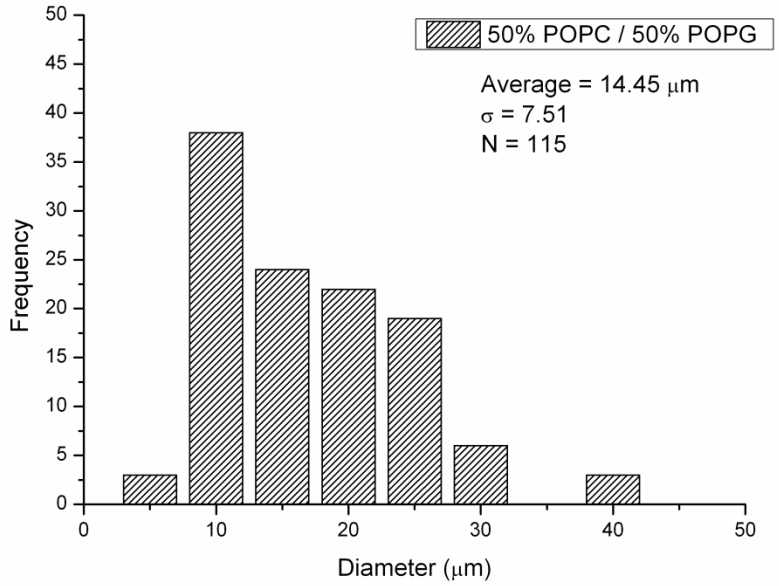

Figure S10. Size distribution of GUVs with lipid composition **D** (50% POPC / 50% POPG) in PBS.

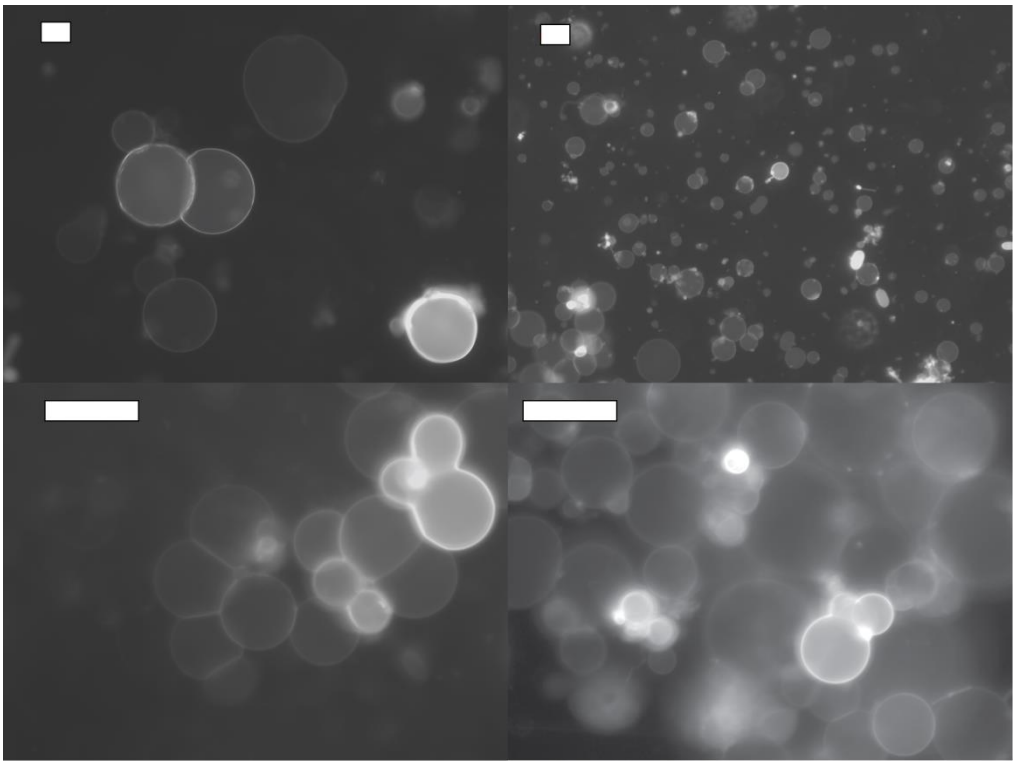

Figure S11. Free floating GUVs formed from **E** (90% POPC / 10% DOPS) in PBS left column and HBS right column. On top 20x magnification and, bottom 63x magnification. The scale bars are 50 μm.

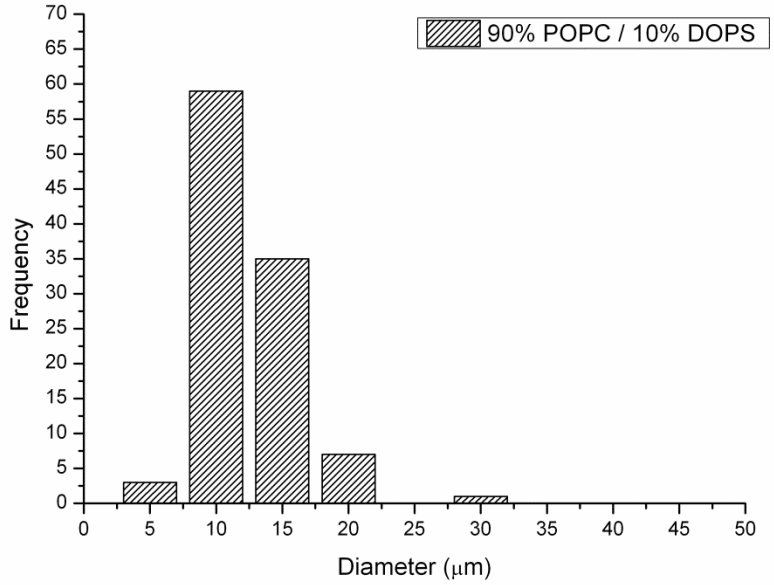

Figure S12. Size distribution of GUVs with lipid composition **E** (90% POPC / 10% DOPS) in PBS.

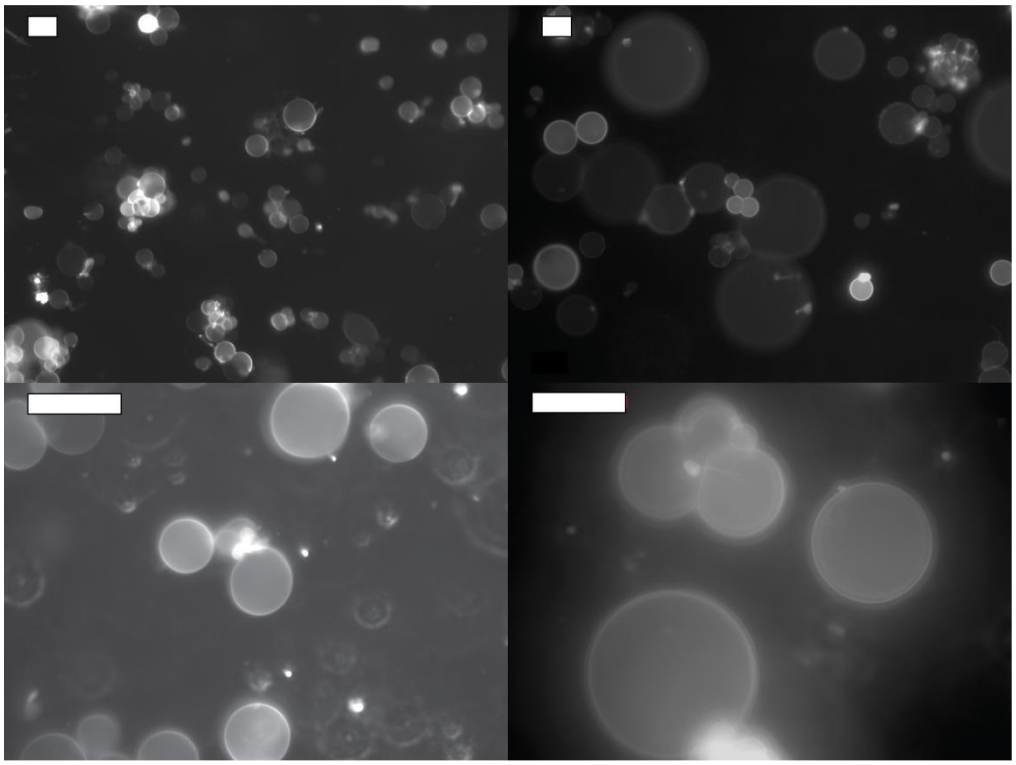

Figure S13. Free floating GUVs formed from **F** (50% DOPC / 25% DOPE / 25% CH) in PBS (left column) and HBS (right column). On top 20x magnification and, bottom 63x magnification. The scale bars are 50 μm.

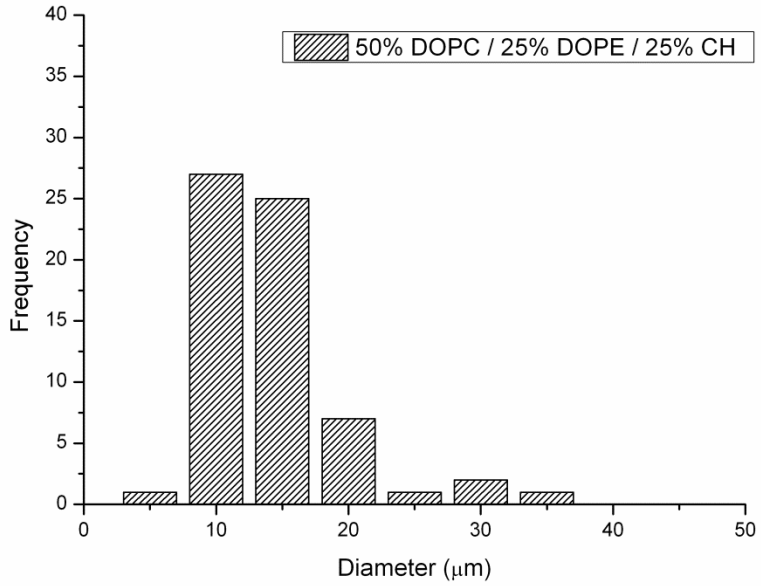

Figure S14. Size distribution of GUVs with lipid composition **F** (50% DOPC / 25% DOPE / 25% CH) in PBS.

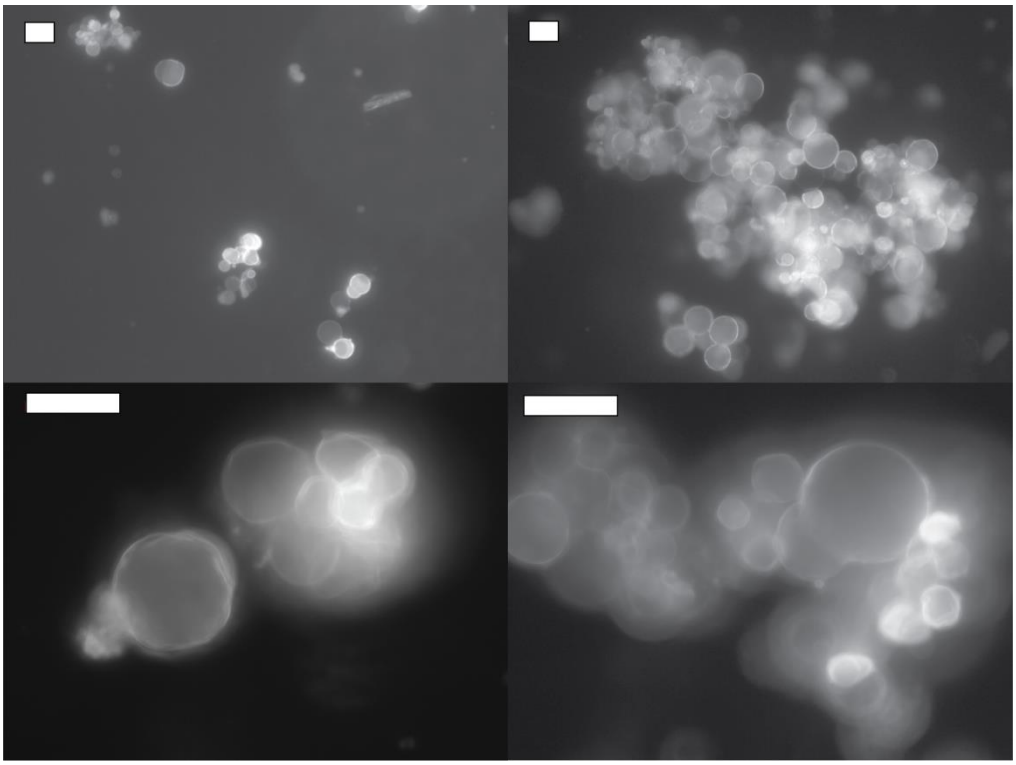

Figure S15. Free floating GUVs formed from **G** (50% DOPC / 50% DPPC) in PBS left column and HBS right column. On top 20x magnification and, bottom 63x magnification. The scale bars are 50 µm.

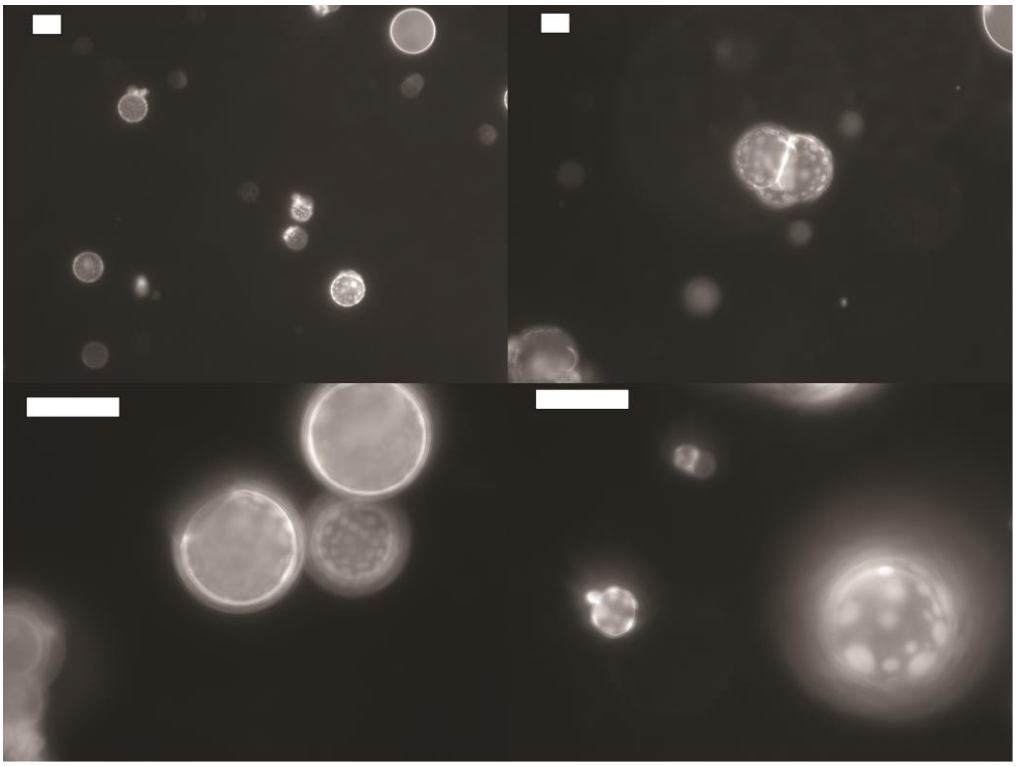

Figure S16. Free floating GUVs formed from **H** (33.3% DOPC / 33.3% DPPC / 33.3% CH) in PBS left column and HBS right column. On top 20x magnification and, bottom 63x magnification. The scale bars are 50 µm.

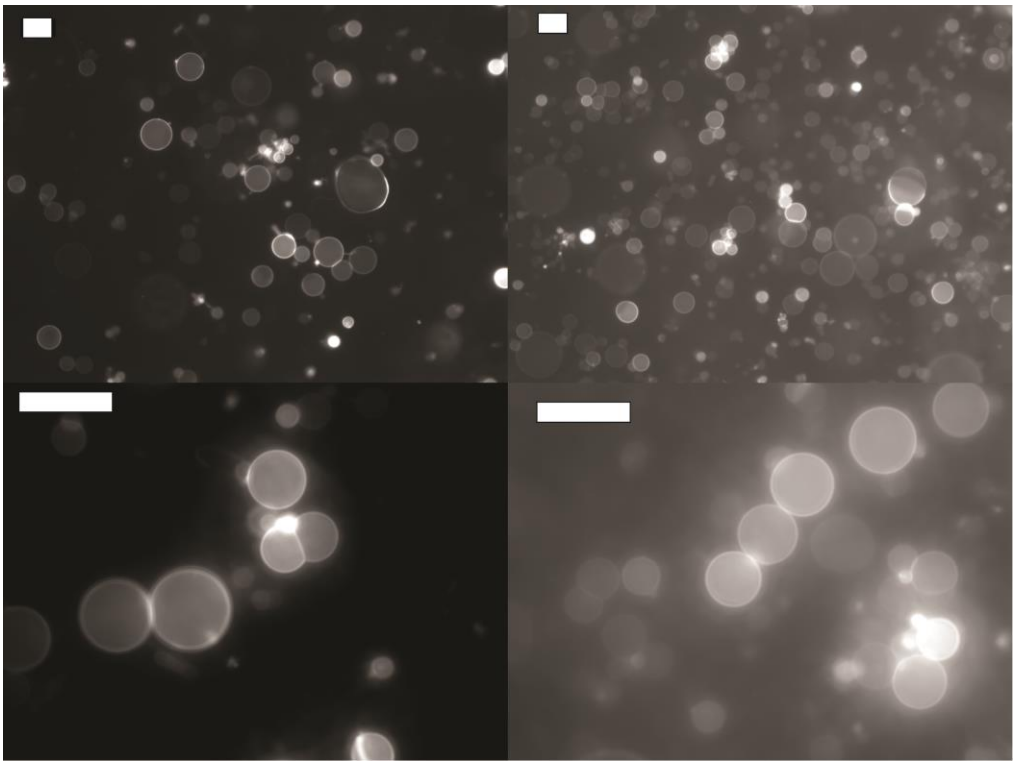

Figure S17. Free floating GUVs formed from **I** (50% DOPC / 20% DOPE / 5% PEG2000-PE / 25% CH) in PBS left column and HBS right column. On top 20x magnification and, bottom 63x magnification. The scale bars are 50 µm.

Dex-Mal was fluorescently labeled (1 and 2.5 % mol) with 7-methoxycoumarin-3-carboxylic acid as fluorescent probe to produce Dex-Mal-C (labeling of molecule **1**). On the right side of ***Figure S18*** the absorption spectra of Dex-Mal-C (2 % weight solution) is presented. The emission spectra of coumarin had a displacement from 402 nm to 410 nm (maximum peak) after labeling (Dex-Mal-C) due to chemical modification.

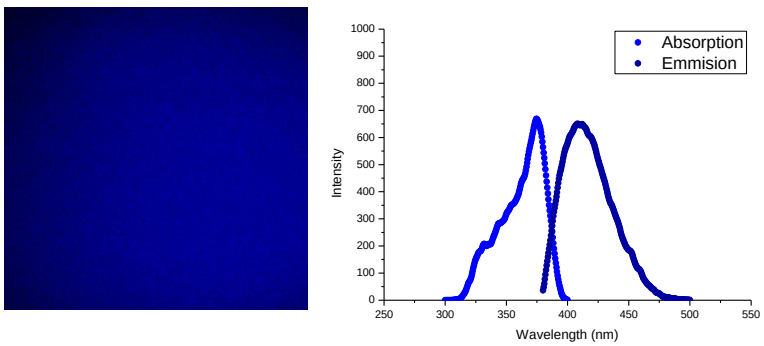

Figure S18. Two Photon Microscopy image of Dex-Mal-C (left) and absorption - emission spectrum of Dex-Mal-C (right) both of them at 2.5 mol % labeling.

Two Photon microscopy (***Figure S18 left***) was used to visualize Dex-PEG-C hydrogel film in a microscope glass slide. The background signal corresponding to none labeled Dex-PEG hydrogel film in a glass slide was subtracted from the signal of Dex-PEG-C image to remove the noise associated to measurement. Similar results were obtained for Dex-PEG-C (1 % mol) labeling. Two photon confocal microscopy was performed to determine the thickness of the hydrogel film in the microscope glass slide. Sectioning of 1 μm was done from the highest to the lowest fluorescence intensity layer. The resulting images are presented in ***Figure S19*** after the background has been subtracted from those measurements. Those images correspond from left to right to the highest fluorescence, the middle fluorescence and non-fluorescence images in the confocal sectioning. The estimated thickness of the film is around 26 μm going from the highest to none fluorescence point.

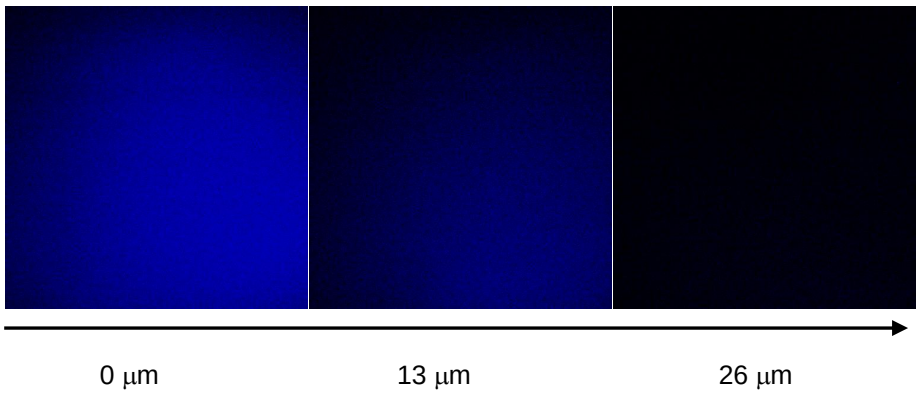

Figure S19. Two photon confocal microscopy images of Dex-PEG-C hydrogel film.

Lipid mixture doped with 0.5 % PE-LR was place on top of a Dex-PEG-C hydrogel film and 1 μm sectioning was made following the previously described procedure. The fluorescence signal was detected by using two photon confocal microscopy in two different channels, one for coumarin and another one for rhodamine. These sequence of images is presented in ***Figure S20*** from highest to lowest intensity layer (right to left). The thickness of the film was measured in 25 μm by doing 1 μm confocal sectioning. The image shows how the doped lipid mixture penetrates the hydrogel network until 15 μm.

Finally, to examine if there is association between Dex-PEG-C and GUVs, two different experiments were performed on Dex-PEG-C hydrogel film. Firstly, GUVs were grown without any fluorescent probe on the lipid mixture. Imaging of non-fluorescent GUVs was performed using phase contrast at 20 x magnification (***Figure S21 A***) and phase contrast at 63 x magnification (***Figure S21 B***). For imaging in epifluorescence mode, a DAPI bandpass filter centered at 450 nm was used to determine the fluorescence of free floating GUVs. The result is presented in ***Figure S21 C*** where non- fluorescence due to coumarin was found either in the membrane or inside GUVs.

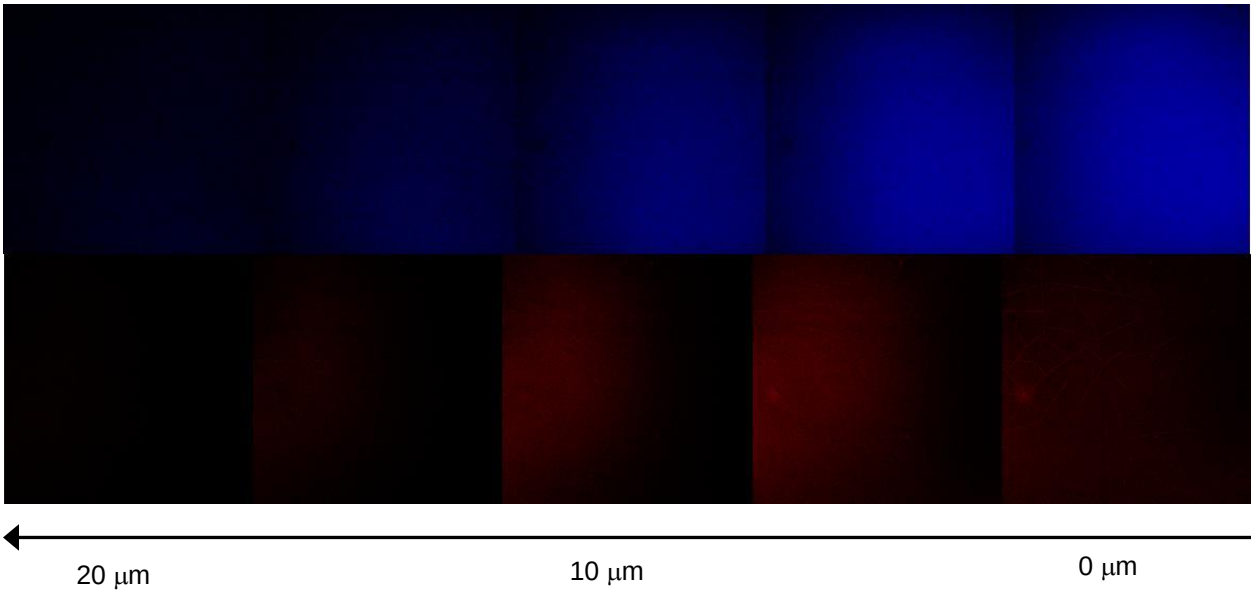

Figure S20. Two Photon Confocal Microscopy of an hybrid film composed of Dex-PEG-C hydrogel and lipid mixture doped with 0.5 mol % PE-LR before immersion in buffer. On top, channel for coumarin and on bottom channel for rhodamine. Each sequence of images corresponds to 5 μm layer sectioning.

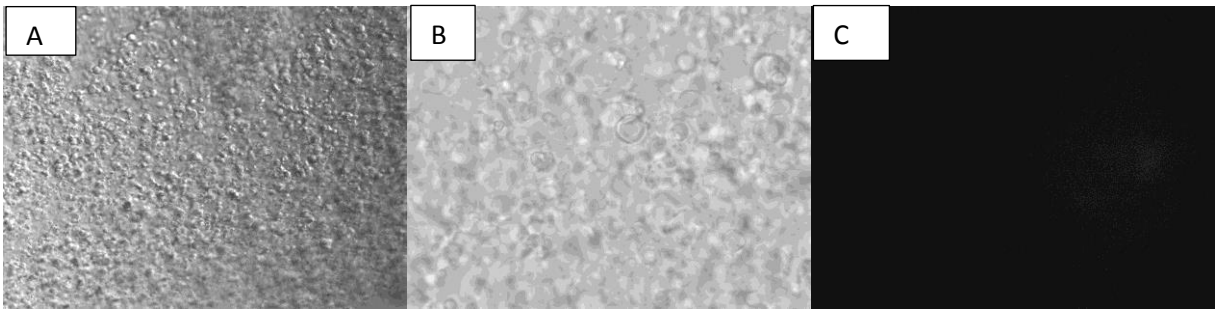

Figure S21. A) Phase contrast microscopy 20 x magnification; ***B)*** Phase contrast microscopy 63 x magnification and, ***C)*** Epifluorescence microscopy using a DAPI bandpass filter centered at 450 nm.

On the other hand, GUVs were grown from lipid mixture doped with 0.5 mol % PE-LR on Dex-PEG-C hydrogel film. A single GUV was imaged in phase contrast microscopy (***Figure S22 A***) and in epifluorescence microscopy using a TRITC filter (***Figure S22 B***); however when the filter was changed to DAPI bandpass filter there was no membrane fluorescence of this GUV (***Figure S22 C***).

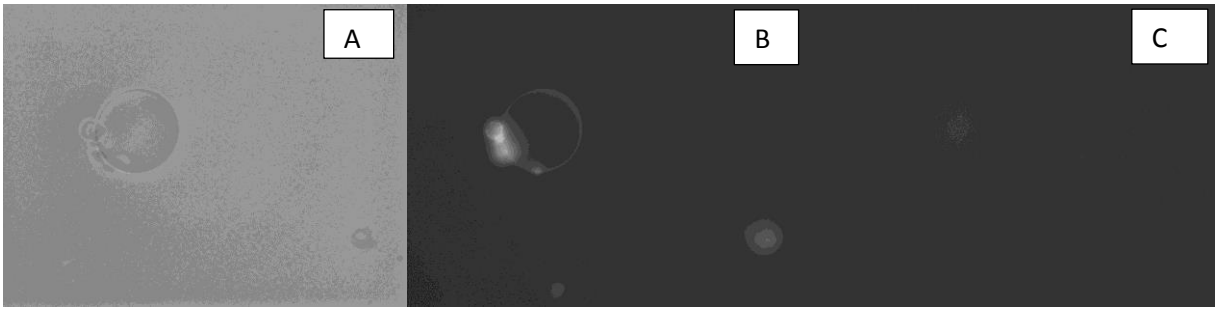

Figure S22. A) Phase contrast microscopy 20 x magnification; ***B)*** Epifluorescence using a TRITC filter and, ***C)*** Epifluorescence using a DAPI bandpass filter.

Even when the lipid mixture penetrates around 15 μm into the hydrogel network, the association between GUVs and Dex-PEG gel was not detected via fluorescence in the membrane or inside the GUVs. The high swelling efficiency of the hydrogel (90 %) which promotes the lamellar repulsion without doping the lipid lamella with none-electrolytic monosaccharides to promote inter-lamellar repulsion produces high yield of GUVs.

BIBLIOGRAPHY

1. R. M. de Figueiredo, P. Oczipka, R. Frohlich and M. Christmann, *Synthesis-Stuttgart*, 2008, 1316-1318.
2. J. S. Moore and S. I. Stupp, *Macromolecules*, 1990, **23**, 65-70.
3. K. Peng, I. Tomatsu, A. V. Korobko and A. Kros, *Soft Matter*, 2010, **6**, 85-87.
4. J. J. Cras, C. A. Rowe-Taitt, D. A. Nivens and F. S. Ligler, *Biosensors and Bioelectronics*, 1999, **14**, 683-688.